Progress In Electromagnetics Research, PIER 57, 33–54, 2006

FIELD STRUCTURES OF WAVEGUIDE JUNCTION CIRCULATORS WITH IRREGULAR SHAPED FERRITE SIMULATED BASED ON EXACT TREATMENT

H. C. Wu and W. B. Dou

State Key Laboratory of Millimeter Waves
Southeast University
Nanjing 210096, China

Abstract—Field structures of waveguide Y-junction circulators containing irregular shaped ferrite material, such as Y-junction with partial-height cylinder/triangle ferrite posts and metal step impedance transformer, Y-junction with a ferrite sphere, and dual higher order modes circulator, which are classified as different junction resonance modes, are depicted to illustrate the circulating process. The analysis method used is a combination of the mode expansion method and finite element method, which is based on the weak form of Helmholtz equation. Calculated results (return loss, insertion loss and isolation) of these structures are shown and compared respectively to those in literatures. Consistencies have been observed.

1. INTRODUCTION

It is well known that waveguide junction circulators are the fundamental elements in microwave and millimeter wave systems. In order to get good performance and eliminate try-and-error method in circulator design, many methods, including MMM [1–5], MoM, FEM [6], BEM, FDTD [7] and etc., have been used to analyze the circulators. However, so far the physical pictures about the circulating process of waveguide junction circulator with different irregular shaped ferrite have not been described in detail based on the exact analysis. The physical picture of the junction circulator circulating is important for practical engineers to understand the circulating mechanism of junction circulator and to design a suitable circulator for meeting requirement of a system. For treatment of various junction circulator structures and drawing the pictures of field structures, a flexible approach that combines finite element method,

which is based on Helmholtz equation weak form, and mode expansion, is used. The Helmholtz equation weak form was introduced by Peterson and Castillo to analyze some two dimensional problems of electromagnetic scattering from inhomogeneous cylinder [8]. Based on the weak form, a final set of linear equations can be acquired by using interpolation to present the electric field and magnetic field in the complicated structure containing anisotropic media, and combining the mode expansion in the regular region to truncate the computing region. Various circulators such as Y-junction circulator with partial-height ferrite cylinder/triangle post and metal step impedance transformer, Y-junction circulator with a ferrite sphere and dual higher order modes circulator are studied. Then E-field distributions in the junction of the circulators are presented to illustrate the circulating process.

2. APPROACH

For the waveguide junction circulator with regular shaped ferrite such as circular post, field in ferrite can be expressed in eigenmodes, the fields in other zones also can be expressed in eigenmodes of the zones, then field matching is done on the interfaces between them so as to get a linear equations. Solving the equations the scattering parameters (S_{ij}) of the junction circulator can be obtained, the treatment procedure has been described in ref. [2] in details. The field in junction is mainly controlled by the field in ferrite material, so knowing the field properties in ferrite is important to know the performance of the circulator. Here, some field expressions in ferrite post are given as follows for describing the circulation of circulator. Field in ferrite post can be expressed by the superposition of eigenmodes. The eigenmodes are classified into two categories: volume modes and surface modes. They are given as followings (only E_z and H_φ are shown here, detail seen ref. [2]):

Volume mode ($0 < k_c^2 < k_f^2\mu_z$):

$$E_z = \sum_n \left[A_{1n}\cos\beta_1 z + A_{2n} ch\beta_2 z\right] J_n(k_c r)\exp(jn\varphi) \tag{1}$$

$$H_\varphi = \sum_n (-j) Y_F \frac{k_c}{k_f}\left\{\left[p_1 J_n'(k_c r) - r_1\frac{nJ_n(k_c r)}{k_c r}\right]\times A_{1n}\cos\beta_1 z + \left[p_2 J_n'(k_c r) - r_2\frac{nJ_n(k_c r)}{k_c r}\right]\times A_{2n} ch\beta_2 z\right\}\exp(jn\varphi) \tag{2}$$

Surface mode ($-\infty < k_c^2 < 0$):

$$E_z = \sum_n \sum_{i=1}^{2} A_{in}\cos\beta_i z I_n(k_c r)\exp(jn\varphi) \tag{3}$$

$$H_\varphi = \sum_i \sum_{n=1}^{2} jY_F \frac{k_c}{k_f} A_{in} \left[p_i I_n'(k_c r) - r_i \frac{n I_n(k_c r)}{k_c r} \right] \cos \beta_i z \exp(jn\varphi) \tag{4}$$

Here,

$$[\mu] = \begin{bmatrix} \mu & -j\kappa & 0 \\ j\kappa & \mu & 0 \\ 0 & 0 & \mu_z \end{bmatrix} \tag{5}$$

$$k_f^2 = \omega^2 \varepsilon_0 \mu_0 \varepsilon_f \tag{6}$$

$$\beta_{1,2}^2 = k_f^2 \mu - k_c^2 \frac{\mu + \mu_z}{2\mu_z} \pm \left[k_c^4 \left(\frac{\mu - \mu_z}{2\mu_z} \right) + \frac{k_f^2 \kappa}{\mu_z} \left(k_f^2 \mu_z - k_c^2 \right) \right]^{1/2} \tag{7}$$

$$p_i = k_f^2 / k_c^2 \tag{8}$$

$$r_i = \frac{\left(k_f^2 \mu_e - k_c^2 - \beta_i^2 \right)}{\kappa k_c^2} \tag{9}$$

$$Y_F = \left(\frac{\varepsilon_0 \varepsilon_f}{\mu_0} \right)^{1/2} \tag{10}$$

k_c is obtained by solving transcend equation, which results from the field matching at interface between ferrite post and dielectric post as shown in Fig. 1. It is detailed in ref. [2]. $J_n(x)$ is Bessel function and $I_n(x)$ is modified Bessel function. And we have $\beta_{vm}^2 < \beta_{sm}^2$, β_{vm} denote the propagation constant of volume mode in z direction and β_{sm} denote that of surface mode. For each structure analyzed in this paper, elements of tensor permeability (5) are specified in appendix.

Surface modes are determined by $I_n(x)$ in the radial direction, so they are non-propagation modes in the radial direction and their field energy is concentrated nearby the cylindrical surface. In z direction the field is determined by triangular function, so it is always oscillation. Because the energy of surface mode always concentrates nearby the ferrite post surface, so the field distribution is not sensitive to the frequency. However, volume modes are determined by $J_n(x)$, so volume modes represent the propagating modes in the radial direction and their energy is concentrated inside the body of ferrite. This field distribution will be changed with frequency changing. However, some volume modes may not be oscillation in z direction as shown in Equation (1). The field expressions out of the ferrite post can be obtained similarly. Details are given in ref. [2].

The circulation of circulator was thought of a resonance of the junction containing ferrite, which is considered a resonator. So the

resonance frequency of the junction is corresponding to the circulating frequency that depends on the ferrite parameters. The resonance mode may be thought of that of a cylinder cavity such as TM_{11} or other resonance modes. So the junction resonance mode is a superposition of many eigenmodes. Different contribution of each eigenmode results in different resonance mode. Changing the ferrite parameters such as size, permittivity and saturated magnetization will results in the changing of contribution of each eigenmode, so the circulating performance is also changed.

In ref. [2] several junction resonance modes of waveguide junction circulator containing ferrite cylinder have been denominated. They are low order modes (C_V-mode, C_{V-S}-mode, C_{S-V}-mode) and higher order modes that are dual higher order modes. All they result from different ferrite size under the condition of same permittivity and saturated magnetization. Both simulation and experimental results of the circulators with ferrite post for different junction modes are also presented. However, the analysis is limited to the circulator with regular ferrite post. And the field structures in junction have not been given there, so we do not know the difference of field structures between them. Here we wish to depict the field structures of waveguide junction circulators with irregular shaped ferrite; it will be useful for practical engineers to understand the circulating process of the circulators and to chose a suitable junction resonance mode to meet the performance requirement of a system. However, the field matching method based on the eigenmode expression is difficult for solving the junction circulator containing irregular shaped ferrite such as triangular ferrite post and ferrite sphere exactly. So another method that will be described in the following section is used. In spite of this, the eigenmode expression is helpful for us to understand the field in junction.

3. HYBRID MODE MATCHING AND FINITE ELEMENT METHOD

Waveguide Y-junction circulator, as show in Figure 1, is taken as an example to show the treatment procedure. Parameter a is the width of the waveguide. The fields are expressed with different functions at different regions.

In the junction with irregular ferrite material (Region I):

$$\vec{E} = \sum_{n=1}^{N} A_n \vec{N}_n(x, y, z) \tag{11}$$

In the waveguide 1 (Region II):

$$\vec{E} = e_{11}^{in}\vec{e}_{11}^{in}(x,y,z) + \sum_{l=1}^{L} e_{1l}^{s}\vec{e}_{1l}^{s}(x,y,z) \tag{12}$$

In the waveguide 2 (Region III):

$$\vec{E} = \sum_{l=1}^{L} e_{2l}^{s}\vec{e}_{2l}^{s}(x,y,z) \tag{13}$$

In the waveguide 3 (Region IV):

$$\vec{E} = \sum_{l=1}^{L} e_{3l}^{s}\vec{e}_{3l}^{s}(x,y,z) \tag{14}$$

Where $\vec{N}_n(x,y,z)$: the first-order edge elements in vector finite element; $\vec{e}_{il}(x,y,z)$: electric vector eigenfunction of the lth mode in the ith waveguide; e_{il}: the coefficient of electric vector eigenfunction of the lth mode in the ith waveguide; A_n: the interpolated value of E at that vector.

Substitute test function $\vec{T}(x,y,z)$ with $\vec{N}_i(x,y,z)$, $i = 1, 2, \cdots, N$ in Helmholtz weak form [9] results in

$$\begin{aligned} &\iiint_I \left[\nabla \times \vec{N}_i \cdot \left(\overline{\overline{\mu}}_r^{-1} \nabla \times \sum_{n=1}^{N} A_n \vec{N}_n\right) - k^2 \vec{N}_i \cdot \left(\overline{\overline{\varepsilon}}_r \sum_{n=1}^{N} A_n \vec{N}_n\right)\right] dV \\ &= -\sum_{j=1}^{3} \iint_{S_j} \vec{N}_i \cdot \left[\hat{n} \times \overline{\overline{\mu}}_r^{-1} \left(\nabla \times \vec{E}\right)\right] dS \end{aligned} \tag{15}$$

Thus N linear equations are obtained. The properties of anisotropic media have been characterized by tensor $\overline{\overline{\mu}}_r^{-1}$ and $\overline{\overline{\varepsilon_r}}$ in (15). For the situation considered here, $\overline{\overline{\mu_r}}$ is equal to $[\mu]$ in Equation (5), and $\overline{\overline{\varepsilon_r}}$ reduced to a scalar quality ε_r. For a lossy anisotropic media $[\mu]$ is given in Appendix, which is easy to implement in (15).

For the fields matching on the interface areas S_j, there exist the following equations:

$$e_{11}^{in}\vec{e}_{11}^{in}(x,y,z) + \sum_{l=1}^{L} e_{1l}^{s}\vec{e}_{1l}^{s}(x,y,z) = \sum_{n=1}^{N} A_n \vec{N}_n \left(x, -\frac{\sqrt{3}}{6}a, z\right) \tag{16}$$

$$\sum_{l=1}^{L} e_{2l}^{s}\vec{e}_{2l}^{s}(x,y,z) = \sum_{n=1}^{N} A_n\vec{N}_n\left(x,\sqrt{3}x+-\frac{\sqrt{3}}{3}a,z\right) \quad (17)$$

$$\sum_{l=1}^{L} e_{3l}^{s}\vec{e}_{3l}^{s}(x,y,z) = \sum_{n=1}^{N} A_n\vec{N}_n\left(x,-\sqrt{3}x+-\frac{\sqrt{3}}{3}a,z\right) \quad (18)$$

By multiplication crossing $\vec{h}_{jl}(x,y,z), l = 1,2,\cdots,L$, on both sides of (16), (17) and (18), and integrating over $S_j, j = 1,2,3$, respectively, $3 * L$ linear equations are gained. Where, $\vec{h}_{il}(x,y,z)$ eigenfunction of the lth mode in the ith waveguide.

Finally, a matrix equation is obtained:

$$AX = B \quad (19)$$

The coefficient matrixes can be expressed as

$$A = \left[\begin{array}{c} [\Gamma]_{N\times N}[C]_{N\times 3L} \\ [D]_{3L\times N}\mathrm{diag}[T]_{3L} \end{array}\right]_{(N+3L)\times(N+3L)},$$

$$B:\ (N+3L)\times 1, \quad X:\ (N+3L)\times 1 \quad (20a)$$

$$[\Gamma]_{ij} = \iiint_I \left[\nabla\times\vec{N}_i\cdot\left(\overline{\overline{\mu}}_r^{-1}\nabla\times\vec{N}_j\right) - k^2\vec{N}_i\cdot\left(\overline{\overline{\varepsilon}}_r\vec{N}_j\right)\right]dV,$$

$$i = 1,2,\ldots,N,\ j = 1,2,\ldots,N \quad (20b)$$

$$[C]_{i[(j-1)^*L+k)]} = \iint_{S_j}\vec{N}_i\cdot\left[\hat{n}\times\overline{\overline{\mu}}_r^{-1}\left(\nabla\times\vec{e}_{jk}^{s}(x,y,z)\right)\right]dS,$$

$$i = 1,2,\ldots,N,\ j = 1,2,3,\ k = 1,2,\ldots,L \quad (20c)$$

$$[D]_{[(i-1)^*L+k)]j} = \iint_{S_i}\vec{N}_j\times\vec{h}_{ik}^{s}(x,y,z)dS,$$

$$i = 1,2,3,\ j = 1,2,\ldots,N,\ k = 1,2,\ldots,L \quad (20d)$$

$$diag\,[T]_{(i^*L+k)} = \iint_{S_i}\vec{e}_{ik}^{s}(x,y,z)\times\vec{h}_{ik}^{s}(x,y,z)dS,$$

$$i = 1,2,3,\ k = 1,2,\ldots,L \quad (20e)$$

$$[B]_i = \begin{cases} \displaystyle\iint_{S_j}\vec{N}_i\cdot\left[\hat{n}\times\overline{\overline{\mu}}_r^{-1}\left(\nabla\times\vec{e}_{11}^{in}(x,y,z)\right)\right]dS & i = 1,2,\ldots,N \\ \displaystyle\iint_{S_i}\vec{e}_{11}^{in}(x,y,z)\times\vec{h}_{11}^{in}(x,y,z)dS & i = N+1 \\ 0 & i = N+1,N+2,\ldots,N+3^*L \end{cases} \quad (20f)$$

X are unknowns to be solved, as shown in followings:

$$X = (A_1, A_2, \ldots, A_N, e^s_{11}, e^s_{12}, \ldots, e^s_{1L}, e^s_{21}, e^s_{22}, \ldots, e^s_{2L}, e^s_{31}, e^s_{32}, \ldots, e^s_{3L})' \tag{20g}$$

$[\Gamma]_{N\times N}$ is acquired by applying N sets of basis functions as testing functions to Eq. (15). $diag[T]_{3L}$ is acquired because of the orthogonality of expansion modes in interfaces. $[C]_{N\times 3L}$ and $[D]_{3L\times N}$ are the results of the field matching on the ports boundary.

Because the plane $z = b/2$ (Parameter b is the height of the waveguide) is a symmetry plane and incident wave is H_{10} mode, it can be considered an electric wall, so only half volume of the junction space need to be considered in calculation. Then for different time t, E-field at plane $z = b/2$ in the junction of the circulator is expressed as:

$$E = \mathrm{Re}\left[\dot{E}_z e^{-j\omega t}\right] \qquad \left(t = \frac{i}{N}\frac{2\pi}{\omega},\ i = 1, 2, \cdots N\right) \tag{21}$$

Usually numerical computation is used to get the scattering parameters of circulators, but the circulating process of the circulators is seldom revealed. Now the field structure is depicted to discover the circulating process or physical mechanism.

4. NUMERICAL RESULTS AND DISCUSSIONS

4.1. Numerical Results for Y-Junction with Partial-Height Ferrite Posts (Lower Junction Resonance Mode: C_{V-S} Mode)

A calculation example of Y-junction circulator with partial-height ferrite post is given in Fig. 2. The field structures from Equation (21) in circulating frequency 36 GHz are depicted in Fig. 3. The ports are corresponding to Fig. 1. Circulation direction is from port 1 to port 2 to port 3. The red circle in the junction denotes the ferrite post. Red region in junction denotes the field in positive value and blue region in negative value.

When $t = 0$ the field in the region near interface $S1$ is positive and in the region near $S2$ is negative, in the region near the mid of port 3 the field is zero, so no power coupled into port 3. Power is transmitted from port 1 to 2, and port 3 is isolated. From the field distribution in different time, we can see the field is rotated because of the action of ferrite post. When $t = 11T/30$ and $12T/30$, although the field in the region near port 3 is positive, the field has been shifted closed to ferrite post, so that the field in $S3$ is still zero and no power is coupled into port 3. When $t = T/2$, the field is the same as that

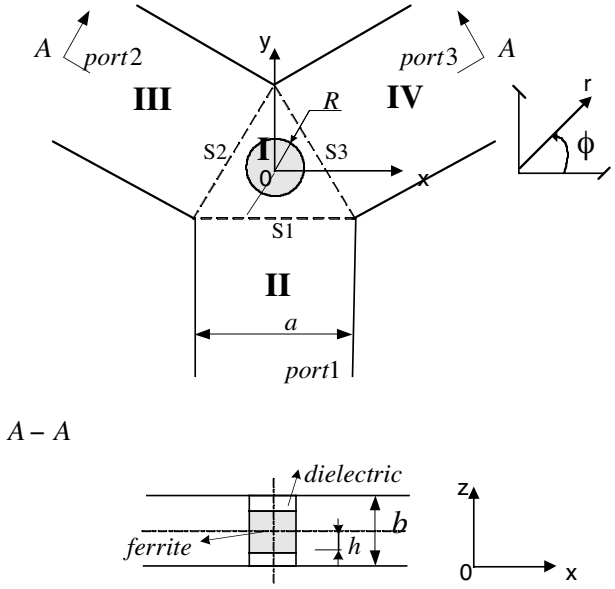

Figure 1. Y-junction circulator loaded with a partial-height ferrite post.

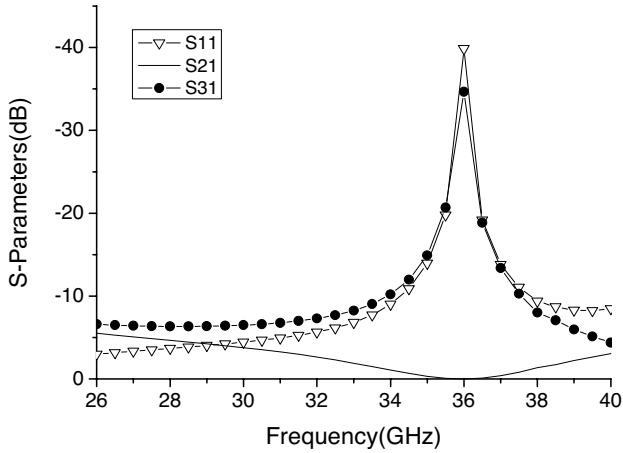

Figure 2. Performance of Y-junction circulator with a partial-height ferrite post $a = 7.12\,\text{mm}$, $b = 3.65\,\text{mm}$, $R/h = 1.1$, $\varepsilon_f = 13.85$, $\varepsilon_d = 2.08$, $H_i = 200\,Oe$, $p = \omega_m/\omega = 0.4$.

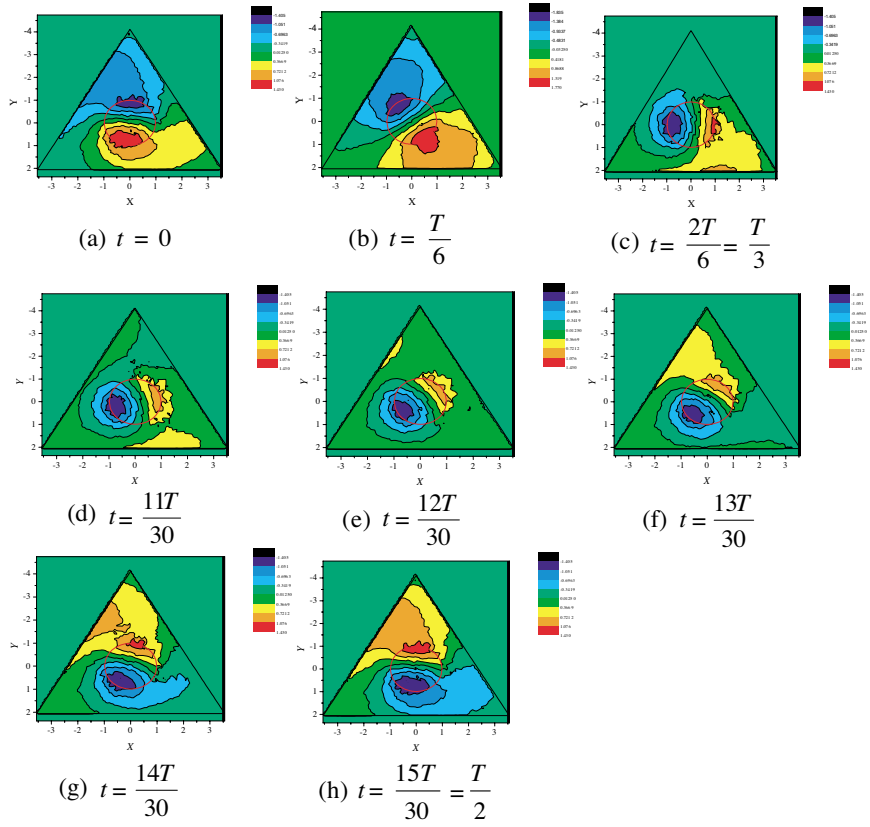

Figure 3. E-field distribution in the junction on plane $z = b/2$ (Frequency: 36 GHz).

in $t = 0$ except the positive and negative value is exchanged. Where $T = 2\pi/\omega$ is time cycle. Therefore, the circulation of circulator is a complex process, which contains field rotation and field shift. In φ. direction field can be distinguished as $n = 1$ mode (here n is equal to the n in eigenmode expressions in Equations (1)–(4)). This junction resonance mode has been denominated as C_{V-S} mode in ref. [2].

4.2. Numerical Results for Y-Junction with Partial-Height Ferrite Cylinder Posts and Metal Step Impedance Transformer (Lower Mode: C_{S-V} Mode)

The configuration of circulator is given in Fig. 4. Fig. 5 shows its performance. Because there are some inhomogeneity of the

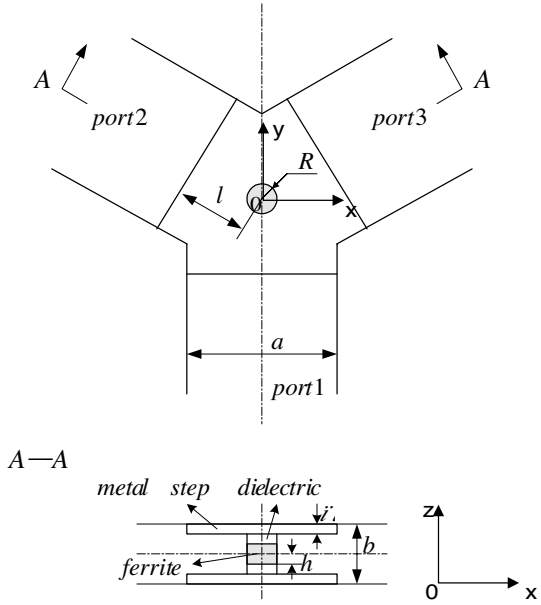

a=7.12 mm, R_0=1.2 mm, h=0.78 mm, δ=0.8 mm,
ε_f =13.85, ε_d=2.08, l=4.05 mm, M_s=0.485T

Figure 4. Schematic diagram of Y-junction circulator with a partial-height cylinder ferrite post and metal step impedance transformer.

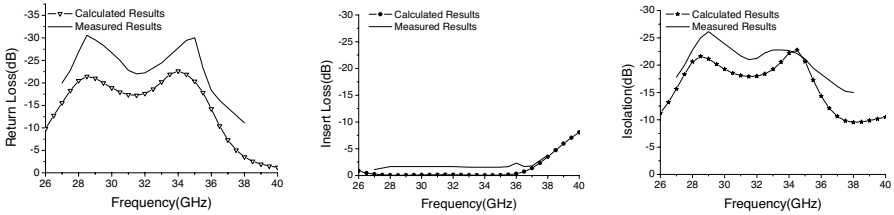

Figure 5. Performance of Y-junction circulator with a partial-height cylinder ferrite post and metal step impedance transformer.

magnetization in ferrite used in the experiment and the error of the manufacture such as the diameter of dielectric piece may be larger a little than that of ferrite post, there is a little difference between the calculation results and measured results. This resonance mode is denominated as C_{S-V} mode in ref. [2]. Because of its broadband performance, the field structures are depicted at two frequencies point and shown in Fig. 6 and Fig. 7, respectively. The circulation process

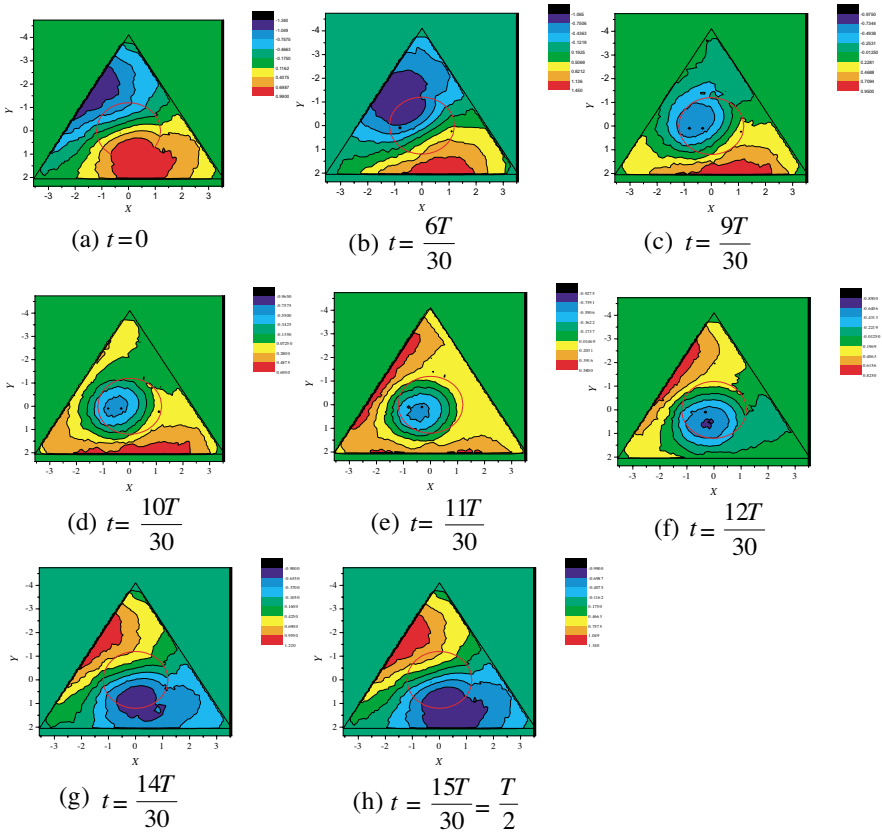

Figure 6. E-field distribution in the junction on plane $z = b/2$ (Frequency: 28.5 GHz).

of mode is different from that of C_{V-S} mode. The field rotation is not obvious. It can be seen from Fig. 6 that the negative value part of field moves from port 2 through mid of junction to port 1 with the time t changing from $6T/30$ through $9T/30$, $10T/30$ and $11T/30$, $12T/30$ to $14T/30$. The positive value part of field moves along the left region of junction around negative part to port 2; that is, negative part seems standing in hall as if a post, positive part circulates around the post from port 1 to port 2 as if stream. From Fig. 7 similar circulation process also can be observed. In φ direction $n = 1$ mode does not clearly displaced as C_{V-S} mode does. It is considered the result of the different contribution of each eigenmode.

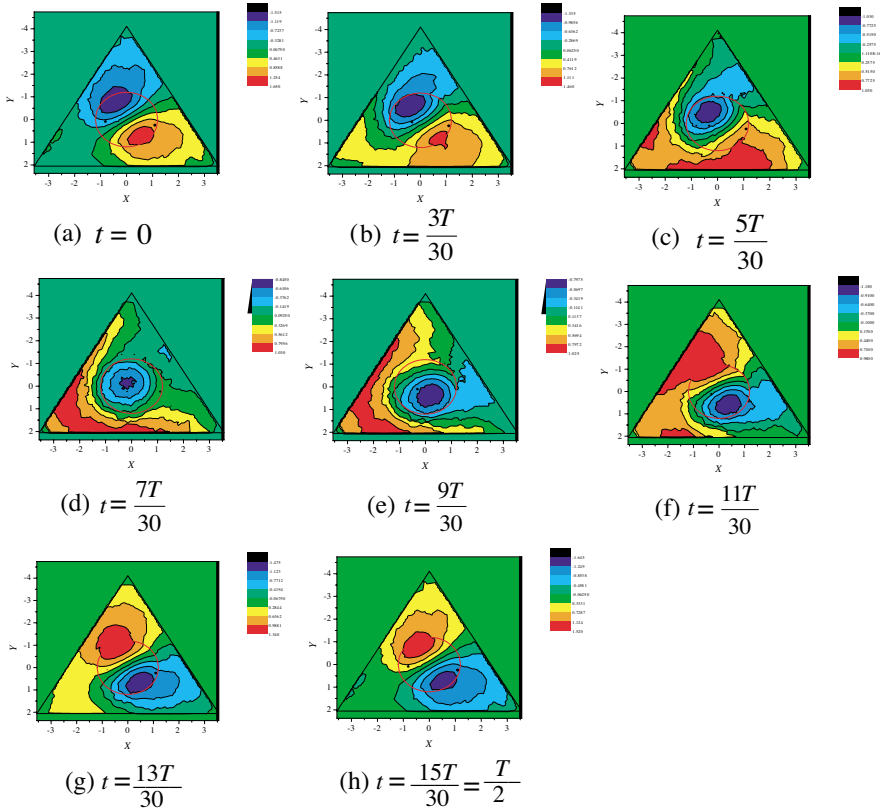

Figure 7. E-field distribution in the junction on plane $z = b/2$ (Frequency: 34 GHz).

4.3. Numerical Results for Y-Junction with Partial-Height Triangle Ferrite Posts and Metal Step Impedance Transformer (Lower Mode: C_{S-V} Mode)

Fig. 8 depicts the configuration of the circulator and Fig. 9 shows the performance. The field structures at circulating frequency are given in Fig. 10. The red triangle line in junction denotes the ferrite. This junction resonance mode may also be denominated as C_{S-V} mode. It can be seen that the negative part of field moves from port 2 to mid of junction then to port 1. The positive part of field moves from port 1 to port 2 along the left of junction around negative part. The circulation process given in Fig. 10 is similar to that given in Fig. 6 and Fig. 7.

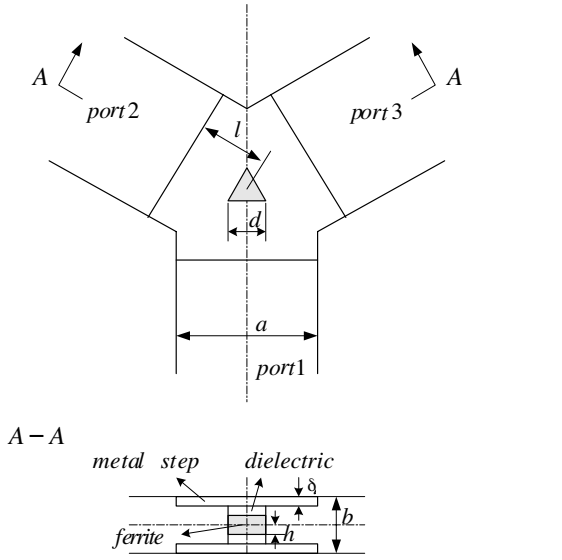

a =7.12 mm, b =3.56 mm, d =3 mm, h =0.93 mm, δ =0.7 mm,
l =4.15 mm, ε_f =13.85, ε_d =2.08, H_i =200Oe, $p = \omega_m / \omega$ =0.4

Figure 8. Y-junction circulator with a partial-height triangle ferrite post and metal step impedance transformer.

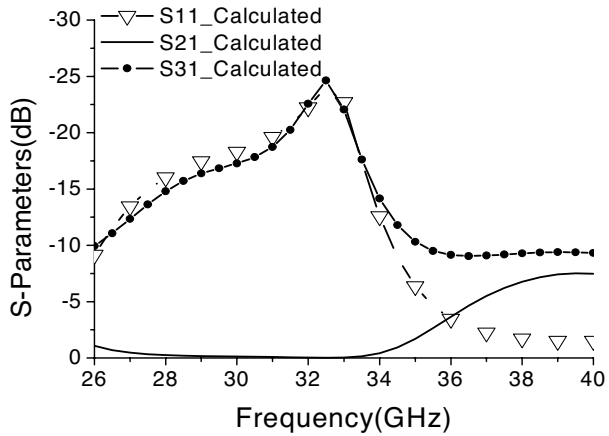

Figure 9. Performance of Y-junction circulator with a partial-height triangle ferrite post and metal step impedance transformer.

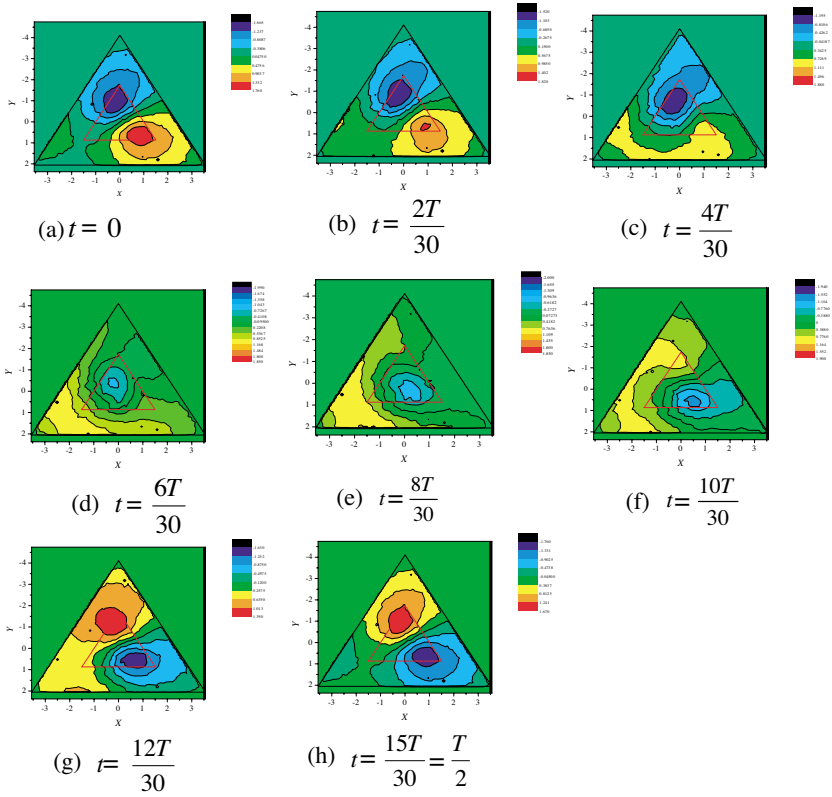

Figure 10. E-field distribution in the junction on plane $z = b/2$ (Frequency: 32.5 GHz).

4.4. Numerical Results for Y-Junction with a Ferrite Sphere (Lower Mode: C_{V-S} Mode)

The configuration of the circulator is shown in Fig. 11. The performance of the circulator is depicted in Fig. 12. Agreement between calculation and experiment has been observed. Also, because of the error of the manufacture such as the ferrite may not be exactly a sphere and the thick or diameter of the two dielectric piece on and below the ferrite sphere may be different, there is a little difference between the calculation results and measured results. It is apparent that the resonance mode of junction containing ferrite sphere may be different from that of junction containing ferrite post. To draw all field components structure in three dimensions is not an easy task. The field structure on the symmetrical plane $z = b/2$ is depicted again as shown

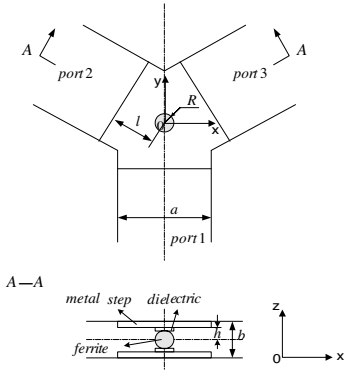

(a) Y-junction circulator

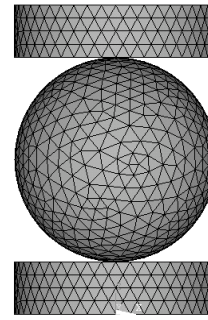

(b) ferrite sphere and dielectric posts (meshed)

$a=2b=2.54$ mm, $R=0.42$ mm, $h=0.635$ mm, $\varepsilon_f=13.5$, $\varepsilon_d=2.25$, $H_i=1700Oe$, $\Delta H=80Oe$, $\tan\delta=2.5\times10^{-4}$, $M_s=0.5T$ this page
$a=2b=2.54$ mm, $R=0.4$ mm $\pm$ 5%, $h=0.635$ mm, $\varepsilon_f=13.5$, $\varepsilon_d=2.25$, $H_i>1700Oe$, $\Delta H<120Oe$, $M_s=0.5T$ in Ref. [10].

Figure 11. Schematic diagram of Y-junction circulator with a ferrite sphere.

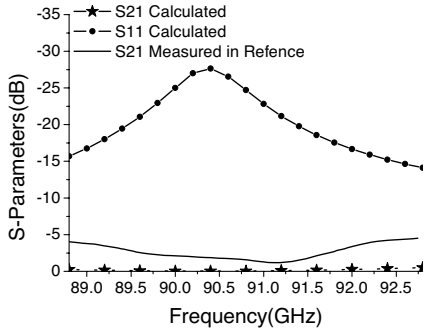

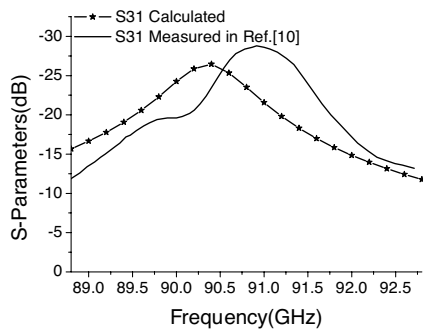

Figure 12. Performance of Y-junction circulator with a ferrite sphere.

in Fig. 13. Take a survey carefully it may be found that the field structure in Fig. 13 is similar at some extent to that in Fig. 3. So it may be called C_{V-S} mode. The field is rotated with time t increasing from $t=0$ to $t=T/2$. When $t=11T/30$, it seems some power may be coupled into port 3. However, the field has been shifted close to the mid of junction, the field along interface $S3$ is zero so no power flows into port 3. In φ direction field can also be distinguished as $n=1$ mode.

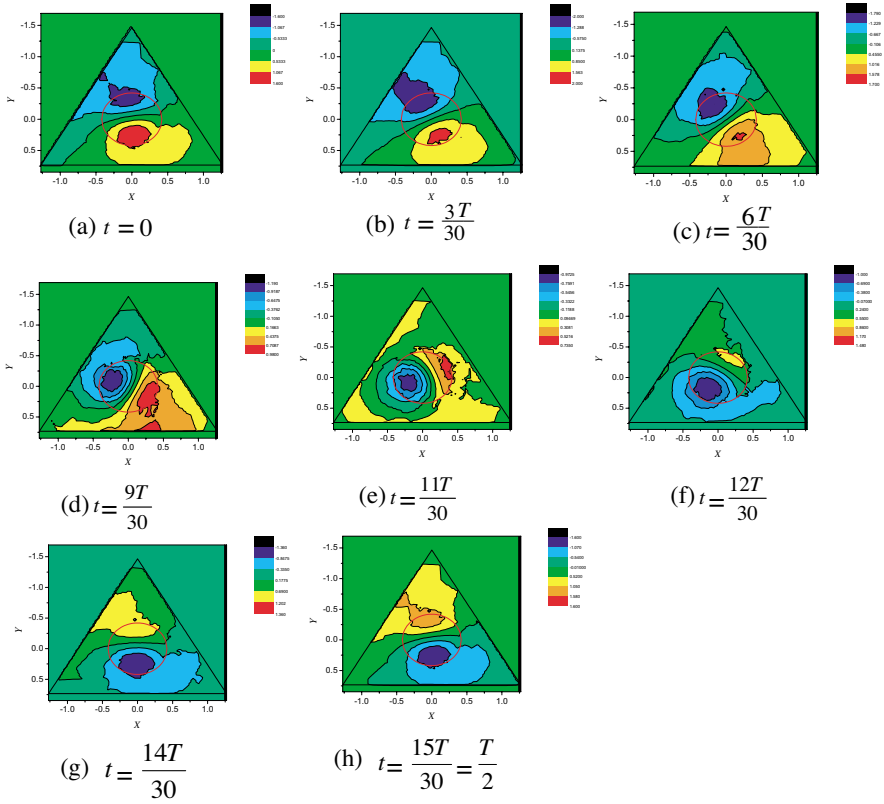

Figure 13. E-field distribution in the junction on plane $z = b/2$ (Frequency: 90.4 GHz).

4.5. Numerical Results for Dual Higher Order Modes Y-Junction Circulators (High Mode: Dual Higher Modes)

Compared to the low order junction resonance mode such as C_{V-S} mode and C_{S-V} mode described above, the higher order resonance modes are supported by large ferrite volume. Usually increasing ferrite radius can get higher order modes. Higher order mode can withstand higher power because it has larger area attached to metal wall of circulator and the height of ferrite piece is small compare to its diameter, so the heat within ferrite can be dissipated through the metal wall more efficiency. At W band the anisotropic action of ferrite is reduced because the saturated magnetization of ferrite can only reach 0.5T, which results in a small value κ of tensor element of ferrite. Therefore, low order mode can only support a

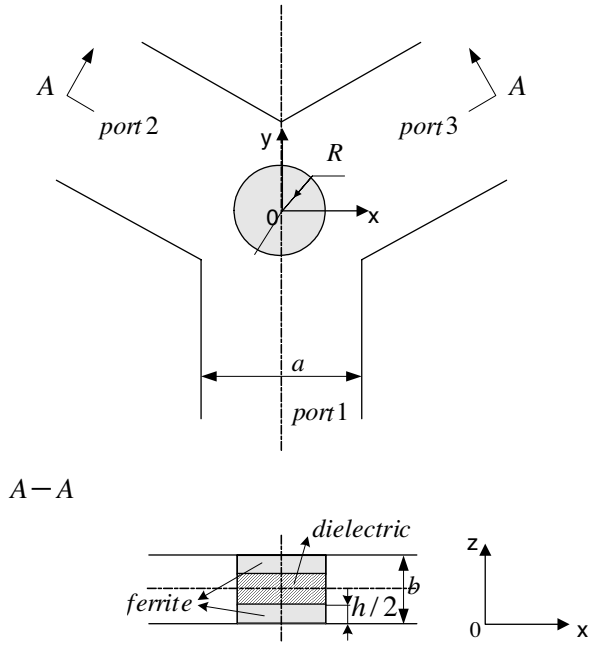

a=2.54 mm, b=1.27 mm, R/h=2.1, ε_f=15.5, ε_d=2.5, H_i=200Oe, $p = \omega_m/\omega$ =0.15

Figure 14. Schematic diagram of dual higher order modes circulator.

narrowband performance, higher order mode can support wider band performance as it has larger ferrite volume to provide anisotropic action. Computation and practices show the higher order mode available is dual higher modes for which two higher order modes circulating in same direction and close to each other, as expounded in ref. [2], an example calculated is shown in Fig. 15. The structure of the circulator is similar to that given in Fig. 1 except ferrite post with larger radius is adopted, which is given in Fig. 14.

First higher order mode circulates in band from 94 GHz to 98 GHz; Second higher order mode circulates from 105 GHz to 107 GHz; from 99 GHz to 103 GHz the circulator has bad performance that can be considered boundary frequency zone between two modes.

Fig. 16 shows the field structure of first higher order mode at 97 GHz where red circular denote the ferrite post. Watching the field structure carefully it can be observed that it displays $n = 2$ mode in φ. direction. When $t = 0$, $3T/30$, $6T/30$ and $9T/30$, it seems that the field near port 3 can excites H_{10} mode in port 3, actually, it excites H_{30} mode; despite the field at mid of interface $S3$ has higher

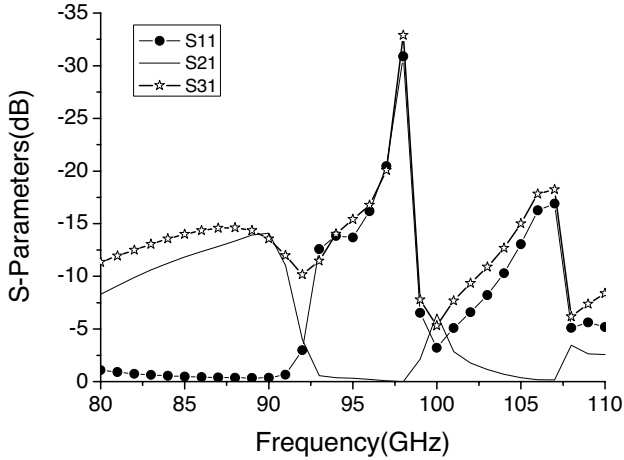

Figure 15. Performance of dual higher order modes circulator.

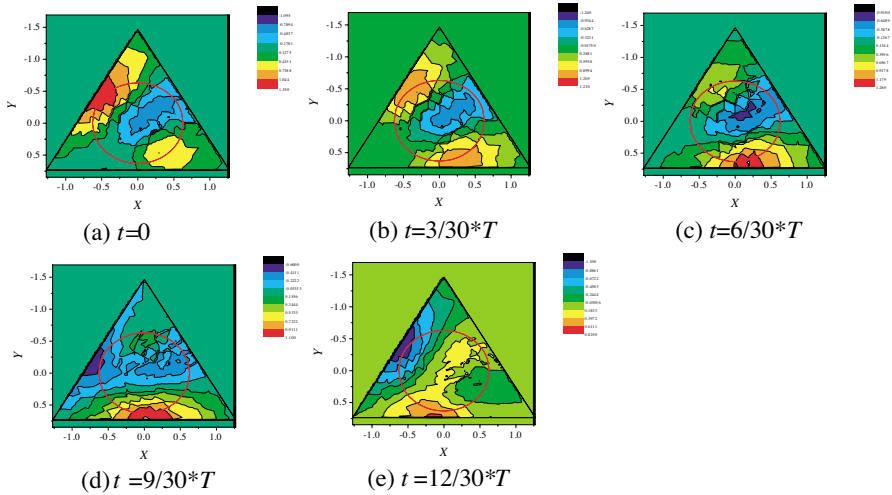

Figure 16. *E*-field distribution in the junction on plane $z = b/2$ (Frequency: 97 GHz).

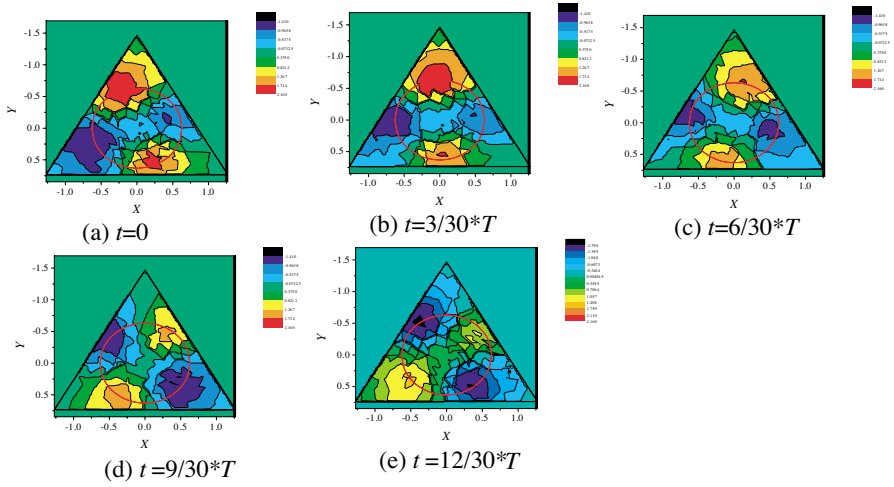

Figure 17. E-field distribution in the junction on plane $z = b/2$ (Frequency: 99 GHz).

negative value, the field at two side of interface $S3$ has positive value, so it excites H_{30} mode other than H_{10} mode. However, H_{30} mode is cutoff in port 3, thus port 3 is isolated. For this high mode the rotation of field structure is not displayed as C_{V-S} mode, and it also is not similar to C_{S-V} mode. When $t = 0$, the power (positive region) enter the junction from port 1, then moves into ferrite post with time increasing. Because the field is dominated by $n = 2$ junction resonance mode, the entered field was distributed through the ferrite post along its diameter as shown in Fig. 16(e) in $t = 12T/30$. When $t = T/2$ the field structure is the same as that in $t = 0$ except the positive region and negative region is exchanged. For the next half cycle from $t = T/2$ to $t = T$, the process is same except the positive region and negative region exchanged.

When frequency is 99 GHz, the field structure is given in Fig. 17 when circulator is not circulating. It display $n = 2$ mode clearly. Entered power was scattered into all 3 ports so the circulator has bad performance. When $t = 0$, the entered power has moved into ferrite post, however, when $t = 3T/30$ and $6T/30$, the power was returned to port 1 a little so the reflect wave in port 1 was excited. When $t = 9T/30$, the transmission wave was excited in port 2. In next half cycle, the transmission wave in port 3 was excited.

The circulation process of second higher order mode, which is given in Fig. 18, is different from first higher order mode. It seems $n = 1$ mode in φ direction. It seems similar to C_{V-S} mode shown

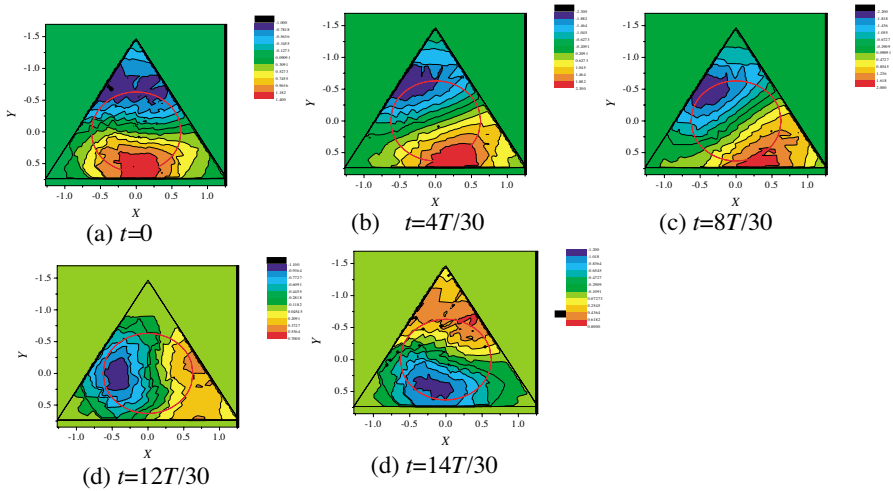

Figure 18. E-field distribution in the junction on plane $z = b/2$ (Frequency: 106 GHz).

in Fig. 3; field structure is rotated with t increasing like C_{V-S} mode, but field was distributed on a larger area like a zoom of C_{V-S} mode, which may results from a larger diameter of ferrite post. When time t changes from $t = 12T/30$ to $14T/30$ the positive region of the field was rotated to port 3, which is not concentrated closed to centre of the junction so some power may leak to port 3 and isolation is degraded.

5. CONCLUSION

Waveguide junction circulators with irregular shaped ferrite are analyzed by a method that combines FEM and mode expansion. The field structures of the circulators are depicted to show the circulation process clearly for the first time. The description on the circulation process is also presented. The correctness of calculation has been confirmed by experiments. These pictures depicted will be helpful for microwave engineers to understand the physical mechanism of waveguide junction circulator and to choose a suitable mode for designing a circulator meeting the requirement of practical system.

APPENDIX A.

Permeability of Ferrite

In ferrite region,

$$\overline{\overline{\mu}}_r = \begin{bmatrix} \mu & j\kappa & 0 \\ -j\kappa & \mu & 0 \\ 0 & 0 & 1 \end{bmatrix} \tag{A1}$$

with

$$\omega_0 = \gamma H_0 \tag{A2}$$

$$\omega_m = \gamma M_s \tag{A3}$$

$$\mu = 1 + \frac{\omega_m \omega_0}{\omega_0^2 - \omega^2} \tag{A4}$$

$$\kappa = \frac{\omega_m \omega}{\omega_0^2 - \omega^2} \tag{A5}$$

where,

γ: the gyromagnetic ratio

M_s: saturated magnetization

H_0: the applied biased dc field

If the ferrite is lossy,

$$\varepsilon_r = \varepsilon_f(1 - j\tan\delta) \tag{A6}$$

$$\mu = \mu' - j\mu'', \qquad \kappa = \kappa' - \kappa'' \tag{A7}$$

$$\mu' = 1 + \frac{\omega_0\omega_m(\omega_0^2 - \omega^2) + \omega_m\omega_0\omega^2\alpha^2}{\left[\omega_0^2 - \omega^2(1+\alpha^2)\right]^2 + 4\omega_0^2\omega^2\alpha^2} \tag{A8}$$

$$\mu'' = \frac{\omega\alpha\omega_m\left[\omega_0^2 + \omega^2(1+\alpha^2)\right]}{\left[\omega_0^2 - \omega^2(1+\alpha^2)\right]^2 + 4\omega_0^2\omega^2\alpha^2} \tag{A9}$$

$$\kappa' = \frac{\omega\omega_m\left[\omega_0^2 - \omega^2(1+\alpha^2)\right]}{\left[\omega_0^2 - \omega^2(1+\alpha^2)\right]^2 + 4\omega_0^2\omega^2\alpha^2} \tag{A10}$$

$$\kappa'' = \frac{2\omega_0\omega_m\omega^2\alpha}{\left[\omega_0^2 - \omega^2(1+\alpha^2)\right]^2 + 4\omega_0^2\omega^2\alpha^2} \tag{A11}$$

$$\alpha = \gamma\Delta H/(2\omega) \tag{A12}$$

Where,

ε_f: dielectric constant of the ferrite

$\tan\delta$: loss tangent

ΔH: ferrite line-width

ACKNOWLEDGMENT

We express our thanks sincerely to the referees for their comments and helpful suggestion that will improve the quality of our paper.

REFERENCES

1. EL-Shandwily, M. E., A. A. Kamal, and E. A. F. Abdallah, "General field theory treatment of H-plane waveguide junction circulators," *IEEE Trans. Microwave Theory Tech.,* Vol. 21, 392–403, Jun. 1973.
2. Dou, W. B. and Z. L. Sun, "Millimeter wave ferrite circulator and rotator," *Int. J. Infrared & MMW,* Vol. 17, 2035–2131, Dec. 1996.
3. Akaiwa, Y., "Mode classification of a triangular ferrite post for Y-circulator operation," *IEEE Trans. Microwave Theory Tech.,* Vol. 25, 59–61, Jan. 1977.
4. Khilla, A. M. and I. Wolff, "Field theory treatment of H-plane waveguide junction with triangular ferrite post," *IEEE Trans. Microwave Theory Tech.,* Vol. 26, 279–287, Apr. 1978.
5. Okamoto, N., "Computer-aided design of H-plane waveguide junction with full-height ferrite of arbitrary shape," *IEEE Trans. Microwave Theory Tech.,* Vol. 27, 315–321, Apr. 1979.
6. Koshiba, M. and M. Suzuki, "Finite-element analysis of H-plane waveguide junction with arbitrarily shaped ferrite post," *IEEE Trans. Microwave Theory Tech.,* Vol. 34, 103–109, Jan. 1986.
7. Hu, S. X. and W. B. Dou, "FDTD analysis of several waveguide junction circulators with full-height ferrite of arbitrary shape," *Int. J. RF and Microwave CAE,* Vol. 14, No. 4, 153–165, 2004.
8. Peterson, A. F. and S. P. Castillo, "A frequency-domain differential equation formulation for electromagnetic scattering from inhomogeneous cylinders," *IEEE Trans. Antennas Propag.,* Vol. 37, 601–607, May 1989.
9. Wu, H. and W. Dou, "Analysis of waveguide multi-ports discontinuities by the helmholtz weak form and mode expansion," *IEEE Proc. Microw. Antennas Propag.,* Vol. 151, 530–536, Dec. 2004.
10. Yung, E. K. N., R. S. Chen, K. Wu, and D. X. Wang, "Analysis and development of millimeter-wave waveguide-junction circulator with a ferrite sphere," *IEEE Trans. Microwave Theory Tech.,* Vol. 46, 1721–1734, Nov. 1998.
11. Jin, J. M., *The Finite Element Method of Electromagnetism,* Xi'dian University Press, Xi'an, 2001 (In Chinese).